

Characterization of TMPRSS2:ETV5 and SLC45A3:ETV5 Gene Fusions in Prostate Cancer

Beth E. Helgeson,¹ Scott A. Tomlins,¹ Nameeta Shah,¹ Bharathi Laxman,¹ Qi Cao,¹ John R. Prensner,¹ Xuhong Cao,¹ Nirmish Singla,¹ James E. Montie,^{2,3} Sooryanarayana Varambally,^{1,3} Rohit Mehra,^{1,3} and Arul M. Chinnaiyan^{1,2,3}

¹Michigan Center for Translational Pathology, Department of Pathology, ²Department of Urology, and ³Comprehensive Cancer Center, University of Michigan Medical School, Ann Arbor, Michigan

Abstract

Recurrent gene fusions involving oncogenic ETS transcription factors (including *ERG*, *ETV1*, and *ETV4*) have been identified in a large fraction of prostate cancers. The most common fusions contain the 5' untranslated region of *TMPRSS2* fused to *ERG*. Recently, we identified additional 5' partners in *ETV1* fusions, including *TMPRSS2*, *SLC45A3*, *HERV-K_22q11.23*, *C15ORF21*, and *HNRPA2B1*. Here, we identify *ETV5* as the fourth ETS family member involved in recurrent gene rearrangements in prostate cancer. Characterization of two cases with *ETV5* outlier expression by RNA ligase-mediated rapid amplification of cDNA ends identified one case with a *TMPRSS2:ETV5* fusion and one case with a *SLC45A3:ETV5* fusion. We confirmed the presence of these fusions by quantitative PCR and fluorescence *in situ* hybridization. *In vitro* recapitulation of *ETV5* overexpression induced invasion in RWPE cells, a benign immortalized prostatic epithelial cell line. Expression profiling and an integrative molecular concepts analysis of RWPE-*ETV5* cells also revealed the induction of an invasive transcriptional program, consistent with *ERG* and *ETV1* overexpression in RWPE cells, emphasizing the functional redundancy of ETS rearrangements. Together, our results suggest that the family of 5' partners previously identified in *ETV1* gene fusions can fuse with other ETS family members, suggesting numerous rare gene fusion permutations in prostate cancer. [Cancer Res 2008;68(1):73–80]

Introduction

Whereas gene fusions are common in hematologic and mesenchymal malignancies, until recently, they have not been well defined in common epithelial tumors. To nominate candidate oncogenes from DNA microarray data, we developed a bioinformatics approach [cancer outlier profile analysis (COPA)] to identify genes with marked overexpression in a subset of cancers (1). COPA identified *ERG* and *ETV1* as prominent "outliers" across multiple prostate cancer data sets. Through several molecular techniques, we identified fusions of the 5' untranslated region (5'-UTR) of *TMPRSS2* (21q22) to *ERG* (21q22) or *ETV1* (7p21) in

cases that overexpressed the respective ETS family member (1). Subsequently, rare fusions of *TMPRSS2* and the ETS family member *ETV4* have also been identified (2, 3). Multiple studies have shown that *TMPRSS2:ERG* fusions are the most predominant subtype of ETS gene fusions (~50% of prostate cancers), and fusions involving *ETV1* or *ETV4* are rare (~1–10% of prostate cancers; refs. 1–7).

More recently, we discovered additional 5' fusion partners involved in *ETV1* gene fusions, including the 5'-UTRs from *SLC45A3*, *HERV-K_22q11.3*, *C15ORF21*, and *HNRPA2B1* (4). Importantly, because these 5' partners are differentially regulated by androgen (androgen-induced, androgen-repressed and androgen insensitive), they define distinct classes of ETS gene rearrangements. To date, these additional 5' partners have only been identified in *ETV1* fusions, and it is unknown if they can fuse with *ERG* (in rare *TMPRSS2:ERG* negative cases with *ERG* outlier expression) or additional ETS family members.

Here we report the discovery of *TMPRSS2:ETV5* and *SLC45A3:ETV5* gene fusions, identifying a fourth ETS family member, *ETV5* (3q27), involved in recurrent gene rearrangements in prostate cancer. This study also shows that the family of 5' fusion partners we previously identified can fuse to additional ETS family members, suggesting numerous rare ETS gene fusion combinations.

Materials and Methods

Samples and cell lines. Prostate tissues were from the radical prostatectomy series and the Rapid Autopsy Program (8), which are both part of the University of Michigan Prostate Cancer Specialized Program of Research Excellence Tissue Core. Samples were collected with informed consent and prior institutional review board approval. The benign immortalized prostate cell line RWPE was obtained from the American Type Culture Collection. Total RNA was isolated from all samples with Trizol (Invitrogen).

***In silico* analysis of *ETV5* outlier expression.** The normalized expression values for *ERG*, *ETV1*, *ETV4*, and *ETV5* from four prostate cancer profiling studies [Glinsky et al. (9), Lapointe et al. (10), Vanaja et al. (11), and Yang et al. (GSE8218)] and this study (X. Cao et al.) in the OncoPrint database (12) were downloaded, and heat maps were generated using Cluster 3.0 and Java Treeview.

Quantitative PCR. Quantitative PCR was done using SYBR Green dye on an Applied Biosystems 7300 Real-time PCR system (Applied Biosystems) as described (1, 2, 4). Oligonucleotide primers were synthesized by Integrated DNA Technologies and are listed in Supplementary Table S1.

RNA ligase-mediated rapid amplification of cDNA ends. RNA ligase-mediated rapid amplification of cDNA ends (RLM-RACE) was done using the GeneRacer RLM-RACE kit (Invitrogen) according to the manufacturer's instructions as described (1, 2, 4). To obtain the 5' end from PCa_ETV5_1, first-strand cDNA was amplified using the GeneRacer 5' primer and ETV5_exon6_racer-r. For amplification from PCa_ETV5_2, ETV5_exon11-r was used.

Note: Supplementary data for this article are available at Cancer Research Online (<http://cancerres.aacrjournals.org/>).

B.E. Helgeson, S.A. Tomlins, and N. Shah contributed equally to this work.

Requests for reprints: Arul M. Chinnaiyan, Department of Pathology, University of Michigan Medical School, 1400 East Medical Center Drive, 5316 CCGC, Ann Arbor, MI 48109-0602. Phone: 734-615-4062; Fax: 734-615-4498; E-mail: arul@umich.edu.

©2008 American Association for Cancer Research.

doi:10.1158/0008-5472.CAN-07-5352

Reverse-transcription PCR. To confirm the expression of *TMPRSS2:ETV5* fusion transcripts in PCa_ETV5_1, we carried out reverse transcription PCR (RT-PCR) as described (1). cDNA was PCR amplified with Platinum Taq High Fidelity using primers for *TMPRSS2:ETV5a/TMPRSS2:ETV5b* and *TMPRSS2:ETV5c* (Supplementary Table S1), and products were resolved by electrophoresis, cloned into pCR4-TOPO, and sequenced as described (1).

Fluorescence *in situ* hybridization. Interphase fluorescence *in situ* hybridization (FISH) on formalin-fixed paraffin-embedded tissue sections was done as described (2, 4). Bacterial artificial chromosomes (listed in Supplementary Table S2) were obtained from the BACPAC Resource Center.

***In vitro* ETV5 overexpression.** Full-length human *ETV5* cDNA (BC007333) in the Gateway compatible vector pDNR-Dual was obtained from the Harvard Institute of Proteomics (HsCD00003658). Adenoviral and lentiviral constructs were generated by recombination with pAD/CMV/V5 (Invitrogen) and pLenti6/CMV/V5 (Invitrogen), respectively, using LR Clonase II (Invitrogen). Control pAD/*LACZ* clones were obtained from Invitrogen and Control pLenti6/*GUS* clones were generated by recombination using a control entry clone (pENTR-*GUS*, Invitrogen). The University of Michigan Vector Core generated the viruses. The benign immortalized prostate cell line RWPE was infected with adenoviruses expressing *ETV5* or *LACZ* and used 48 h after infection. RWPE cells were also infected with lentiviruses expressing *ETV5* or *GUS*, and stable clones were generated by selection with blasticidin (Invitrogen). *ETV5* expression was confirmed by immunoblotting with a mouse monoclonal anti-*ETV5* antibody (Abnova) at 1:500 dilution. Mouse monoclonal anti-glyceraldehyde-3-phosphate dehydrogenase (*GAPDH*) antibody (Abcam) was applied at 1:30,000 dilution for loading control.

Invasion assays. Invasion assays were done as described (4). Equal numbers of the indicated cells were seeded onto basement membrane matrix (extracellular matrix, Chemicon) present in the insert of a 24-well culture plate, with fetal bovine serum added to the lower chamber as a chemoattractant. After 48 h, noninvading cells and extracellular matrix were removed with a cotton swab.

For inhibitor studies, amiloride (20 $\mu\text{mol/L}$, EMD Biosciences); matrix metalloproteinase (MMP)-3, MMP2/MMP9, MMP8, and the pan-MMP inhibitor GM 6001 (all 10 $\mu\text{mol/L}$, EMD Biosciences); or vehicle control was added to cells for 24 h before trypsinization and seeding for invasion assays, as described above. For plasminogen activator inhibitor (PAI)-1, cells were trypsinized and treated with the indicated amount of recombinant PAI-1 (EMD Biosciences) for 15 min at indicated concentrations before seeding, as described above.

Expression profiling. Expression profiling of transient RWPE-*ETV5* and RWPE-*LACZ* cells was done using the Agilent Whole Human Genome Oligo Microarray as described with a dye flip hybridization (4). Overexpressed and underexpressed signatures were generated by filtering to include only features with significant differential expression ($P_{\log \text{ ratio}} < 0.01$) in both hybridizations after correction for a dye flip. Signatures were loaded into the Oncomine Concepts Map⁴ for analysis as described (4, 13, 14).

Results and Discussion

In this study, we applied COPA to an expression profiling data set generated as part of an integrative molecular study of prostate cancer progression.⁵ Consistent with previous profiling studies, in this data set, COPA identified *ERG* as the second ranking outlier at the 90th percentile and *ETV1* as the 61st outlier at the 95th percentile. Intriguingly, COPA ranked another ETS family member, *ETV5*, as the 4th ranking outlier at the 95th percentile, with 2 of 12 (17%) localized cancers showing outlier expression (noted as PCa_ETV5_1 and PCa_ETV5_2; Fig. 1A). Whereas one of the two

samples concurrently showed *ERG* outlier expression, the other sample did not overexpress *ERG* or *ETV1* (Fig. 2).

Because our original application of COPA did not identify *ETV5* as an outlier in prostate cancer profiling studies (1), we hypothesized that the 17% prevalence in localized prostate cancers in this study was an overestimate of the true prevalence of *ETV5* outlier expression. Thus, we examined *ETV5* expression across several prostate cancer profiling data sets in the Oncomine database, revealing only two additional cases with *ETV5* outlier expression [total, 4 of 269 (~1.5%); Fig. 2], suggesting that *ETV5* outlier expression is indeed rare, similar to *ETV4* (~1.1%; Fig. 2). To confirm both the *ETV5* outlier expression in our two samples and the rarity of *ETV5* outlier expression, we carried out quantitative PCR on samples from our expression profiling data set as well as 44 additional localized prostate cancers. This analysis confirmed *ETV5* outlier expression in PCa_ETV5_1 and PCa_ETV5_2, whereas the additional screen of 44 prostate cancers revealed no further *ETV5* outlier cases (Fig. 1B). Together, these results suggest that similar to *ETV4*, *ETV5* outlier expression is rare in prostate cancer.

In previous studies, >95% of cases with *ERG* or *ETV1* outlier expression harbored chromosomal rearrangements (1, 2, 4, 15), suggesting that rearrangements similarly cause *ETV5* outlier expression. Previously, we used an exon-walking quantitative PCR strategy that showed loss of outlier expression at the 5' end of the ETS transcript in cases that harbored gene fusions (1, 2). Using 10 primer pairs across the 13 exons in the *ETV5* transcript, we found outlier expression of *ETV5* exons 2 to 13 in PCa_ETV5_1 and *ETV5* exons 8 to 13 in PCa_ETV5_2 (Fig. 1C). Thus, to identify a potential 5' partner, we carried out RLM-RACE, which identified three products in PCa_ETV5_1 and one product in PCa_ETV5_2. Sequencing of the PCa_ETV5_1 products showed three different *TMPRSS2:ETV5* fusions (*TMPRSS2:ETV5a-TMPRSS2:ETV5c*; Fig. 3A). The *TMPRSS2:ETV5a* transcript contained exon 1 of *TMPRSS2* fused to exon 2 of *ETV5* and *TMPRSS2:ETV5b* contained exons 1 to 3 of *TMPRSS2* fused to exon 2 of *ETV5*. In the *TMPRSS2:ETV5c* transcript, sequencing revealed a distinct 1st exon and exons 2 to 3 of *TMPRSS2* fused to exon 2 of *ETV5*. This 1st exon is ~1.5 kb downstream of the reference sequence 1st exon and overlaps with a reported EST (DA460061; Supplementary Fig. S1).

Sequencing of the PCa_ETV5_2 RLM-RACE product revealed exon 1 of *SLC45A3* fused to exon 8 of *ETV5* (Fig. 3A). Recently, we identified *SLC45A3* as a 5' fusion partner in *ETV1* gene rearrangements (4). Our discovery of the *SLC45A3:ETV5* fusion confirms *SLC45A3* as another recurrent 5' partner in ETS gene fusions and suggests that the other 5' fusion partners may be involved in additional rare ETS rearrangements. Together, RLM-RACE of both cases confirmed the exon-walking quantitative PCR expression patterns and shows the existence of *ETV5* gene fusions in prostate cancers with *ETV5* outlier expression.

To confirm the presence of the fusion transcripts found in PCa_ETV5_1 and PCa_ETV5_2, we carried out quantitative PCR. As shown in Fig. 3B, quantitative PCR detected *TMPRSS2:ETV5b/c* exclusively in PCa_ETV5_1 and *SLC45A3:ETV5* in PCa_ETV5_2. To confirm the expression of individual *TMPRSS2:ETV5* isoforms in PCa_ETV5_1, we carried out RT-PCR using primers specific for *TMPRSS2:ETV5a/TMPRSS2:ETV5b* and *TMPRSS2:ETV5c*. Sequencing of amplified products using *TMPRSS2:ETV5a/TMPRSS2:ETV5b* primers confirmed the expression of both *TMPRSS2:ETV5a* and *TMPRSS2:ETV5b* (Supplementary Fig. S2). PCR using primers for *TMPRSS2:ETV5c* produced two products, which were identified as

⁴ <http://www.oncomine.org>

⁵ X. Cao et al., in preparation.

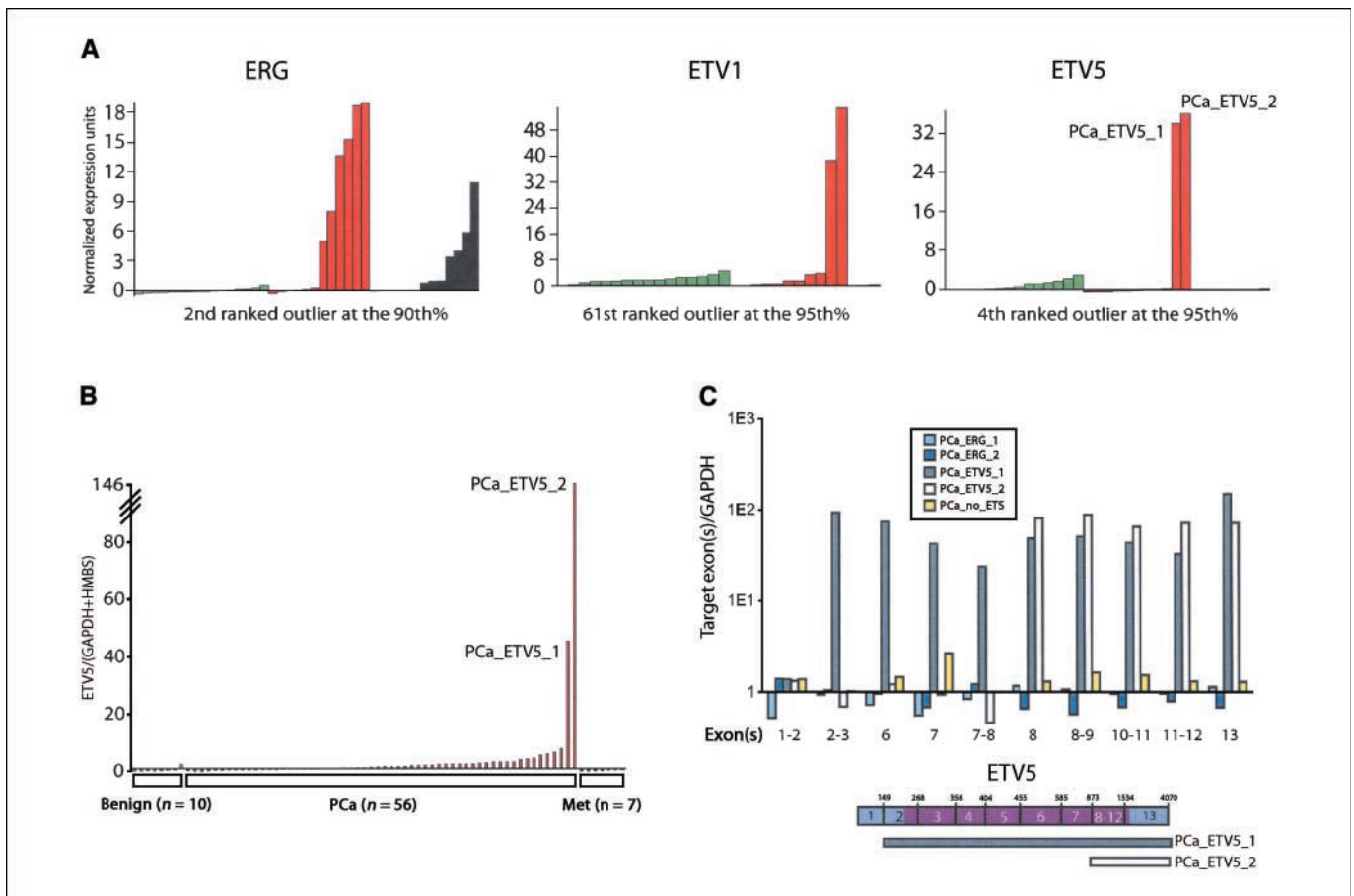


Figure 1. *ETV5* exon expression in prostate cancers with outlier expression. **A**, applying the bioinformatics algorithm COPA to our prostate cancer expression profiling data set identified the ETS family members *ERG*, *ETV1*, and *ETV5* as high-ranking outliers. The expression of each gene in benign prostate (green), clinically localized prostate cancer (red), and metastatic prostate cancer (black) in normalized expression units is indicated. For each gene, the COPA ranking at the indicated percentile from this study is indicated. *ETV5* outliers (PCa_ETV5_1 and PCa_ETV5_2) are indicated. **B**, *ETV5* expression was measured by quantitative PCR in our expression profiling data set ($n = 29$) plus an additional 44 clinically localized prostate cancers. In total, we assayed 10 benign prostate tissue samples (green), 56 localized prostate cancers (PCa; red), and seven metastatic prostate cancers (Met; black). Relative quantities of the *ETV5* transcript in each sample were normalized to the average of *GAPDH* and *HMBS*. The relative amount of *ETV5* was calibrated to the median of all samples. *ETV5* outliers identified in **A** are indicated. **C**, quantitative PCR was used to determine the relative expression of *ETV5* exons in prostate cancers with *ERG* overexpression (PCa_ERG_1 and PCa_ERG_2), a prostate cancer that was negative for ETS overexpression (PCa_no_ETS), and PCa_ETV5_1 and PCa_ETV5_2. Exon(s) measured by the respective primer pair are indicated below the graph. Relative quantities of each exon were normalized to the average of *GAPDH*. The relative amount of *ETV5* exons in each sample was calibrated to the median of the five prostate cancers. A schematic of the noncoding (light purple) and coding (dark purple; start codon in exon 2) regions of *ETV5* are shown; the numbers above the exons (indicated by boxes) indicate the last base of each exon. The gray and white bars below the schematic represent the overexpressed exons in PCa_ETV5_1 and PCa_ETV5_2, respectively.

TMPRSS2:ETV5c and *TMPRSS2:ETV5d*, another isoform containing the novel 1st exon of *TMPRSS2* (found in *TMPRSS2:ETV5c*) fused to exon 2 of *ETV5* (Fig. 3A and Supplementary Fig. S2).

Next, to confirm these fusions at the genomic level, we carried out FISH using split signal assays around the 5' partners (*TMPRSS2* and *SLC45A3*) as well as fusion assays (5' *TMPRSS2* or *SLC45A3* and 3' *ETV5*; Fig. 3C). In PCa_ETV5_1, multiple hybridizations failed to produce interpretable signals for *TMPRSS2*, *ETV5*, or *ERG* probes (positive control) because the only tumor cells in the tissue section were present in a small focus at the extreme edge. Review of all blocks from the case failed to yield more informative sections. However, in PCa_ETV5_2, we confirmed rearrangements in *SLC45A3* and *ETV5* and fusion of the 5' *SLC45A3* and 3' *ETV5* signals (Fig. 3C). Together, quantitative PCR and RT-PCR validated the presence of *TMPRSS2:ETV5* and *SLC45A3:ETV5* in PCa_ETV5_1 and PCa_ETV5_2, respectively, and FISH confirmed the fusion of the *SLC45A3* and *ETV5* genomic loci in PCa_ETV5_2.

In previous studies, we and others have shown that *ERG* and *ETV1* mediate invasiveness in prostate cancer cell lines harboring ETS rearrangements and benign prostate cell lines ectopically overexpressing ETS family members (4, 16).⁶ Thus, we recapitulated *ETV5* overexpression *in vitro* to determine its role in prostate cancer. We generated adenoviruses and lentiviruses expressing *ETV5* and infected the immortalized benign prostate cell line RWPE to generate transient and stable RWPE-*ETV5* cells, respectively (Fig. 4A). Transient and stable *ETV5* overexpression in RWPE cells had no effect on proliferation (data not shown); however, we observed increased invasion through a modified basement membrane assay in RWPE-*ETV5* cells compared with control infected RWPE cells [transient, 4.7-fold ($P = 0.0006$); stable, 4.8-fold ($P = 0.0008$); Fig. 4A].

⁶ S.A. Tomlins et al., submitted for publication.

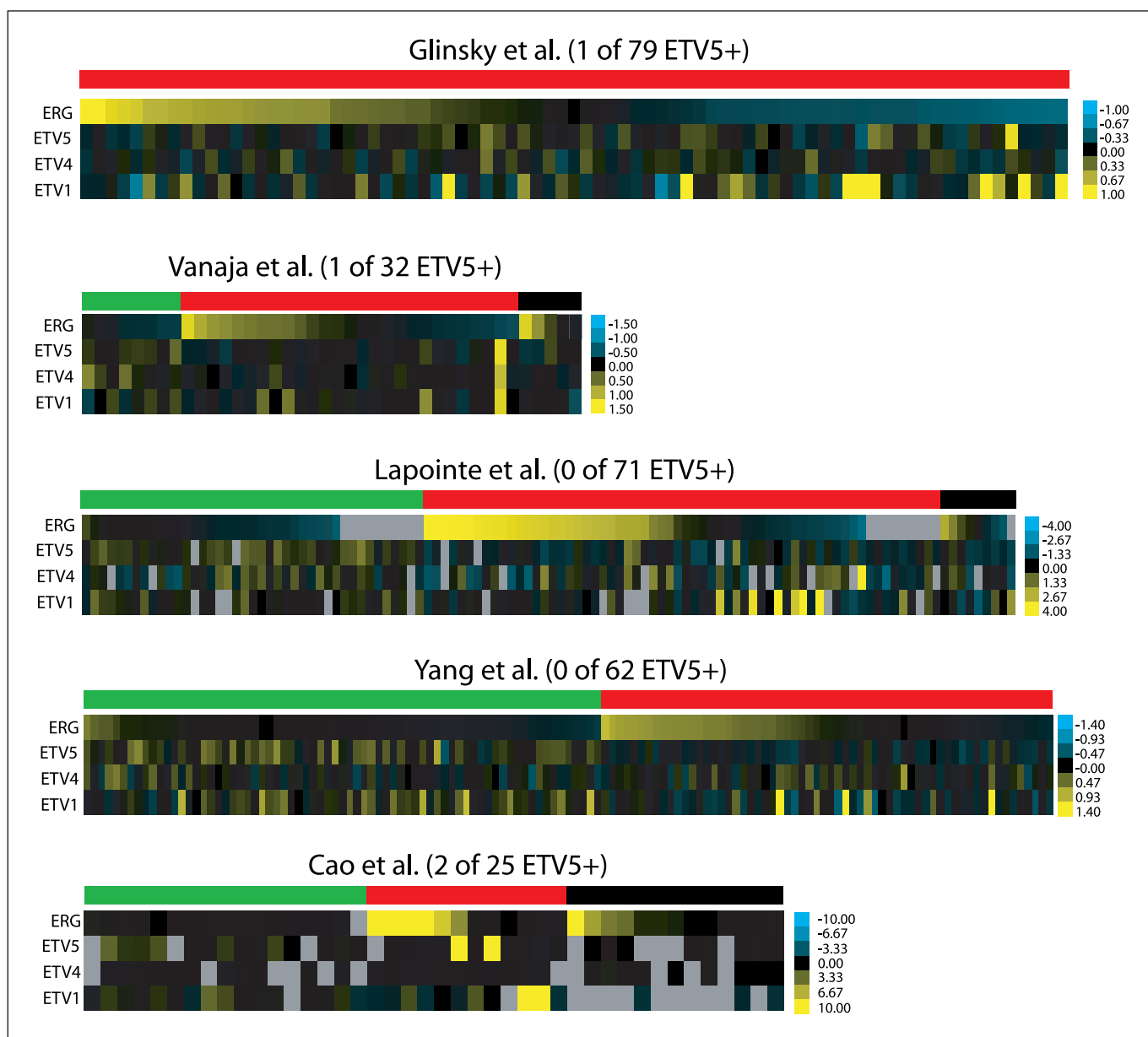


Figure 2. Expression of *ERG*, *ETV1*, *ETV4*, and *ETV5* in prostate cancer profiling studies. The expression of *ERG*, *ETV1*, *ETV4*, and *ETV5* in five prostate cancer profiling studies from the OncoPrint database was used to generate heat maps. Rows, genes; columns, benign prostate tissue samples (green), localized prostate cancers (red), and metastatic prostate cancers (black). Yellow and blue, relative overexpression and underexpression, respectively, according to the color scale. Gray cells, features that did not pass filtering. The number of *ETV5* outliers in each study is indicated after the last name of the first author.

To investigate the transcriptional program regulated by *ETV5* overexpression, we profiled transient RWPE-*ETV5* cells and analyzed the expression signatures using the OncoPrint Concepts Map,⁴ a tool for analyzing associations between >20,000 biologically related gene sets by disproportionate overlap (13, 14). Previously, OncoPrint Concepts Map analysis has identified enrichment of concepts related to invasion in our “overexpressed in RWPE-*ERG* or RWPE-*ETV1*” signatures, consistent with the phenotypes of these cells (4).⁶ We identified 420 features overexpressed in transient RWPE-*ETV5* compared with RWPE-*LACZ* cells.

Whereas we observed enrichment of our “overexpressed in RWPE-*ERG* or RWPE-*ETV1*” concepts in our “overexpressed in RWPE-*ETV5*” signature (Fig. 4B), we unexpectedly observed more

significant enrichment with our “underexpressed in RWPE-*ERG* or RWPE-*ETV1*” signatures. For example, our underexpressed and overexpressed in RWPE-*ERG* (transient) signatures were both enriched in our overexpressed in RWPE-*ETV5* signature (OR, 7.97 and 2.45; $P = 1.3e-25$ and $5e-4$, respectively). Because distinct subsets of genes overexpressed in RWPE-*ETV5* cells were both overexpressed and underexpressed in RWPE-*ERG* and RWPE-*ETV1* cells, this suggests that *ETV5*, *ERG*, and *ETV1* differentially regulate a common set of target genes when overexpressed in benign prostate cells.

Importantly, OncoPrint Concepts Map analysis identified a network of invasion related concepts that shared enrichment with our overexpressed in RWPE-*ETV5*, RWPE-*ERG*, and RWPE-*ETV1*

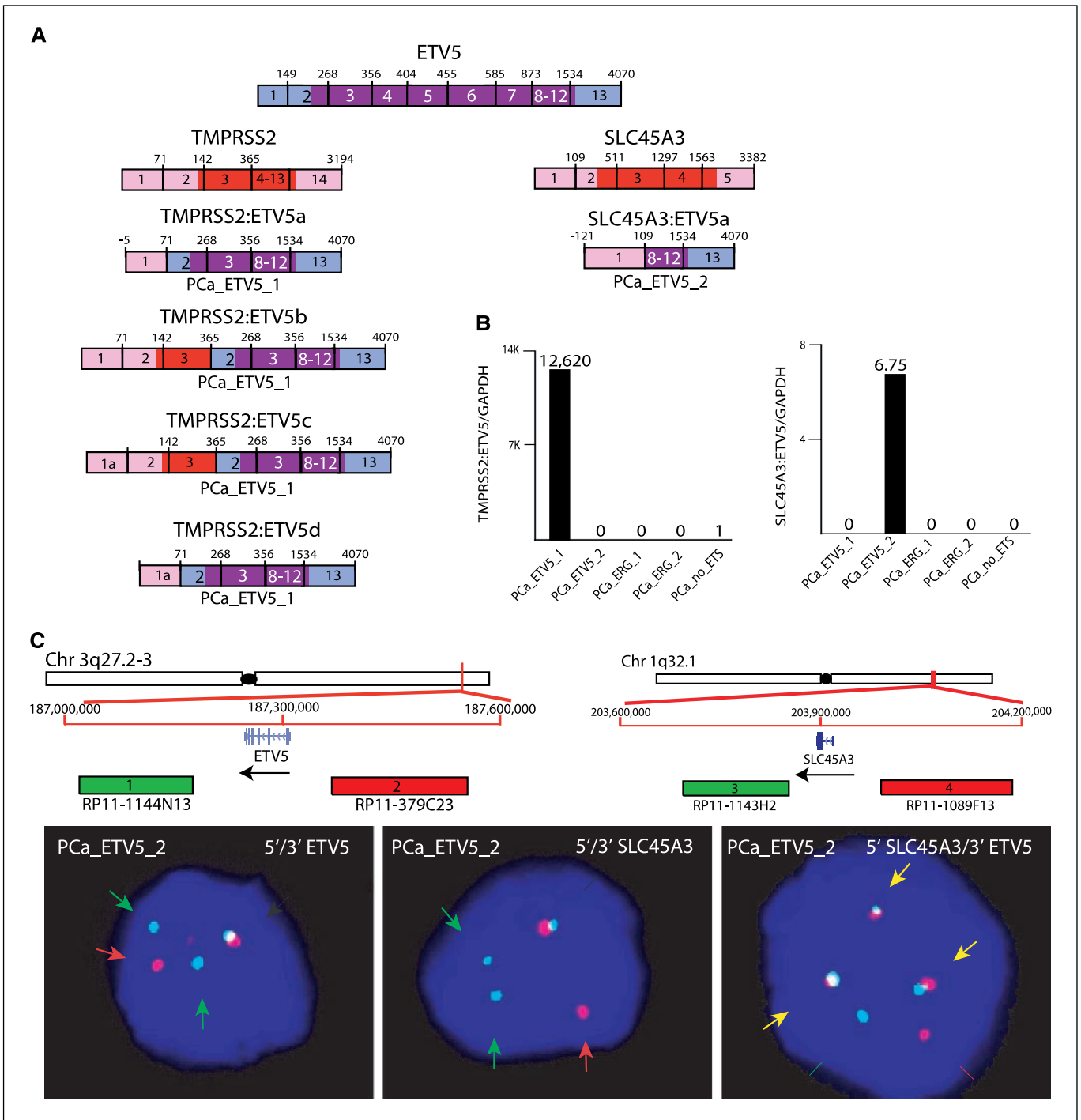


Figure 3. Fusion of *TMPRSS2* and *SLC45A3* to *ETV5* in prostate cancers. **A**, RLM-RACE was used to characterize the complete *ETV5* transcript in PCa_ETV5_1 and PCa_ETV5_2. Sequencing revealed three distinct *TMPRSS2:ETV5* transcripts in PCa_ETV5_1 and one *SLC45A3:ETV5* transcript in PCa_ETV5_2. An additional *TMPRSS2:ETV5* isoform (*TMPRSS2:ETV5d*) identified by RT-PCR is also shown. Structures for *ETV5* (purple), *TMPRSS2* (red), and *SLC45A3* (red) reference sequences are shown. The numbers above the exons (indicated by boxes) indicate the last base of each exon. Untranslated regions are shown in corresponding lighter shades. Identified fusions are colored and numbered from the original reference sequences. **B**, the expression of *TMPRSS2:ETV5* and *SLC45A3:ETV5* fusion transcripts was confirmed by quantitative PCR. Samples used for *ETV5* exon expression in Fig. 1C were assayed for *TMPRSS2:ETV5b/c* and *SLC45A3:ETV5* fusion transcripts by quantitative PCR. Relative quantities of the respective fusion transcript were normalized to *GAPDH*, and the relative amount of each fusion transcript was calibrated to the second highest expressing sample (if any samples showed background amplification). Calibrated quantities are indicated, and samples without detectable fusion transcript after 36 cycles of amplification are indicated by a null value. **C**, FISH was done to confirm *ETV5* and *SLC45A3* rearrangements and *SLC45A3:ETV5* fusion in PCa_ETV5_2. Schematics of bacterial artificial chromosomes located 5' and 3' to *ETV5* and *SLC45A3* that were used as probes for interphase FISH are shown. Chromosomal coordinates are from the March 2006 build of the human genome using the University of California Santa Cruz Genome Browser. Bacterial artificial chromosomes are indicated as numbered rectangles. Genes are shown with the direction of transcription indicated by the arrowhead and exons indicated by bars. FISH was done using bacterial artificial chromosomes as indicated with the corresponding fluorescent label on PCa_ETV5_2. Sections were assayed for split 5'/3' signals of *ETV5* (left) and *SLC45A3* (middle) and the fusion of 5' *SLC45A3* and 3' *ETV5* signals (right). Red and green arrows, split signals; yellow arrows, fused signals.

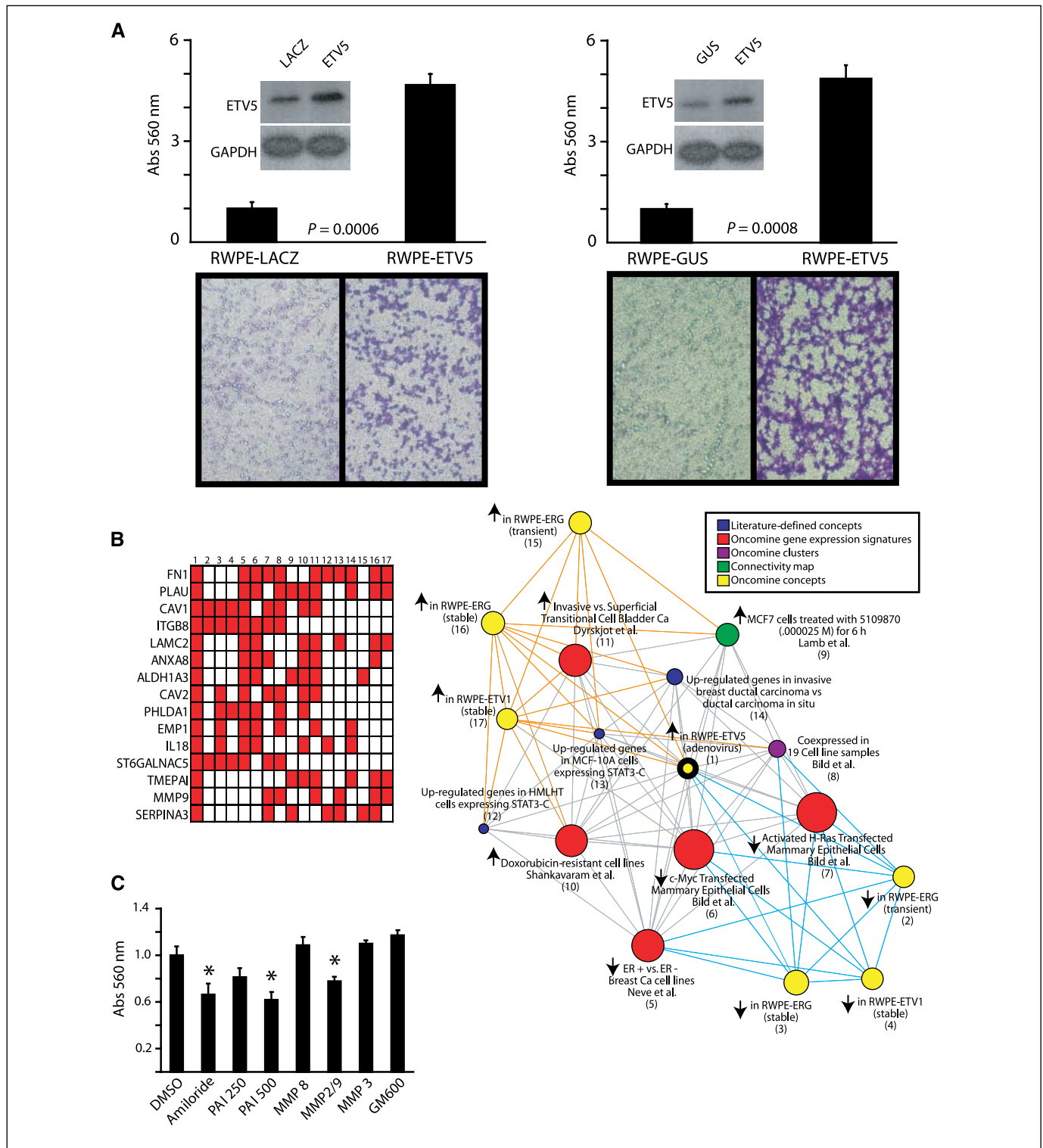


Figure 4. Overexpression of *ETV5* in benign immortalized prostate cells induces invasion. **A**, the benign immortalized prostate cell line RWPE was infected with an adenovirus expressing *ETV5* or *LACZ* control (left) or a lentivirus expressing *ETV5* or *GUS* control (right) and cells were assayed for invasion through a modified basement membrane assay [mean ($n = 3$) + SE]. Immunoblotting confirmation of *ETV5* overexpression and photomicrographs of invaded cells as indicated are shown. Representative of three independent experiments. **B**, transient overexpressing RWPE-*ETV5* and RWPE-*LACZ* cells were profiled on Agilent Whole Genome microarrays and expression signatures were loaded into the OncoPrint Concept Map. Molecular concept map analysis of the overexpressed in RWPE-*ETV5* compared with RWPE-*LACZ* signature (ringed yellow node). Each node represents a molecular concept or a set of biologically related genes. The node size is proportional to the number of genes in the concept. The concept color indicates the concept type according to the legend. Each edge represents a significant enrichment ($P < 5e-4$). Enrichments involving concepts representing overexpressed and underexpressed in RWPE cells expressing *ERG* or *ETV1* signatures are shown in orange and cyan, respectively. *Inset*, an overlay map identifying genes present (red cells) across multiple concepts in the overexpressed in RWPE-*ETV5* enrichment network (indicated by number). **C**, RWPE-*ETV5* cells were treated with the *PLAU* inhibitor amiloride, the *PLAU* and *PLAT* inhibitor PAI-1, or MMP inhibitors (including the pan-MMP inhibitor GM-6001) as indicated and assayed for invasion as in **A**.

concepts, such as “up-regulated genes in HMLHT (or MCF-10A) breast cells expressing STAT3-C” (OR, 5.38; $P = 9.9e-5$). In HMLHT and MCF-10A cells, ectopic expression of *STAT3-C* resulted in increased invasion in a *MMP9*-dependent manner without effecting proliferation (17). Importantly, we observed overexpression of *MMP9* and *PLAU* in RWPE-*ETV5* cells, as we have previously shown that *ERG*-mediated invasion in RWPE cells is inhibited by amiloride, a specific inhibitor of *PLAU*, and PAI-1, a *PLAU* and *PLAT* inhibitor.⁶ In this study, we show that amiloride, PAI-1, and a *MMP2/MMP9* inhibitor inhibit *ETV5*-mediated invasion (Fig. 4C). Together, the overlapping target genes of *ERG*, *ETV1*, and *ETV5* support the functional redundancy of ETS rearrangements in prostate cancer.

ETV1, *ETV4*, and *ETV5* compose the PEA3 subfamily of ETS genes. Members of this subfamily share a highly conserved ETS binding domain (~95% amino acid homology) and are almost 50% identical along the full protein (18). In this study, COPA identified *ETV5* as an outlier in our prostate cancer expression profiling microarray data set. In this data set, the incidence of *ETV5* overexpression was ~17% (2 of 12 localized prostate cancers), but an *in silico* screen of 269 prostate cancer cases and quantitative PCR analysis of an additional 44 prostate cancers revealed *ETV5* overexpression in ~1% (4 of 313) of cases, similar to *ETV4*. Our work here shows that all PEA3 subfamily members are involved in rare ETS rearrangements in prostate cancer (only 1–8% of cases), with the increased prevalence of *ERG* fusions possibly due to the proximity of *ERG* and *TMPRSS2* on chromosome 21.

We and others have shown *TMPRSS2* to be a 5' fusion partner for all ETS genes with known rearrangements (1–6, 19–21). Consistent with previous *TMPRSS2* fusions to *ERG*, *ETV1*, or *ETV4*, where several isoforms have been reported per case (1, 6, 20, 22), here we identified four *TMPRSS2:ETV5* isoforms in PCa_ETV5_1. In most ETS fusions, the 5' partner does not contribute to the coding sequence of the fusion transcript, suggesting the production of a truncated ETS protein and the importance of the promoter region of the 5' partner in driving ETS gene outlier expression. In *TMPRSS2:ETV5a*, exon 1 of *TMPRSS2* is fused to *ETV5* at exon 2, allowing for production of the full-length *ETV5* protein (reported start codons of *TMPRSS2* and *ETV5* are in exons 2 and 2, respectively; see Fig. 3A). Alternatively, *TMPRSS2:ETV5b* and *TMPRSS2:ETV5c* transcripts contain the start codon for *TMPRSS2* in frame with the untranslated and coding sequence of *ETV5*, possibly resulting in the production of a fusion protein. Importantly, expression of *TMPRSS2:ERG* isoforms that encode a fusion production has been associated with more aggressive prostate cancers (20). Additional *ETV5* fusion positive cancers will need to be characterized to determine if chimeric protein coding *ETV5* fusions are similarly aggressive.

Additionally, the *TMPRSS2:ETV5c/d* transcripts contained a distinct 1st exon compared with the 1st exon of the reported

TMPRSS2 reference sequence. This 1st exon in our *TMPRSS2:ETV5c/TMPRSS2:ETV5d* transcripts is ~1.5 kb downstream of the reference sequence 1st exon and overlaps with the EST DA460061, which was originally found in a tongue tumor library (Supplementary Fig. S1). Distinct sequences of *TMPRSS2* involved in ETS gene fusions have been found by other studies. Recently, Lapointe et al. showed that 34 of 63 (54%) cases expressed a novel 1st exon of *TMPRSS2* that is ~4 kb upstream of the reference sequence and overlaps with three ESTs (DA872508, DA868984, and DA870830; ref. 6; Supplementary Fig. S1). In addition, Lapointe et al. (6) report the same 1st exon in *TMPRSS2* that we found in our *TMPRSS2:ETV5c* transcript in a single *TMPRSS2:ERG* case. Additionally, the *TMPRSS2:ETV4* rearrangement showed two fusion transcripts that each contained a novel 1st exon of *TMPRSS2* that is ~8 kb upstream of the reported reference sequence (ref. 2, Supplementary Fig. S1). Together, these results support our hypothesis that the dysregulation of ETS family members is driven by androgen response elements within the upstream sequence of *TMPRSS2* and other previously identified 5' partners. Whereas we were unable to show the *TMPRSS2:ETV5* fusion at the genomic level using FISH due to lack of tissue, the presence of multiple splice variants in other *TMPRSS2:ETS* gene fusions confirmed by FISH suggests that the transcripts are produced as the result of a chromosomal rearrangement rather than *trans*-splicing.

We recently discovered novel 5' fusion partners to *ETV1*, including *SLC45A3*, *HERV-K_22q11.23*, *C15ORF21*, and *HNRPA2B1*. In this study, by applying COPA to a prostate cancer profiling data set, we identified rare *ETV5* gene fusions with two different 5' partners, *TMPRSS2* and *SLC45A3*. Ectopic overexpression of *ETV5* in benign prostate cells induced invasion and an invasive transcriptional program that is analogous to that seen with the overexpression of *ERG* and *ETV1*. Collectively, this study identifies novel ETS gene fusions involving the third member of the PEA3 subfamily, *ETV5*, and shows that the family of 5' partners can fuse to multiple ETS family members, supporting the existence of multiple rare ETS gene fusions.

Acknowledgments

Received 9/14/2007; revised 10/27/2007; accepted 10/30/2007.

Grant support: Department of Defense grant PC040517 (no. W81XWH-06-1-0224; R. Mehra); NIH Prostate Specialized Program of Research Excellence grants P50CA69568 and R01 CA102872; Early Detection Research Network grant UO1 CA11275-01; the Prostate Cancer Foundation; a sponsored research agreement from Gen-Probe, Inc.; Clinical Translational Research Award from the Burroughs Wellcome Foundation (A.M. Chinnaiyan); and a Rackham Predoctoral Fellowship (S.A. Tomlins). S.A. Tomlins is a Fellow of the Medical Scientist Training Program.

The costs of publication of this article were defrayed in part by the payment of page charges. This article must therefore be hereby marked *advertisement* in accordance with 18 U.S.C. Section 1734 solely to indicate this fact.

We thank S. Dhanasekaran, J. Siddiqui, M. LeBlanc, L. Wang, A. Menon, and B. Han for technical assistance, and the University of Michigan Vector Core for virus generation.

References

- Tomlins SA, Rhodes DR, Permer S, et al. Recurrent fusion of *TMPRSS2* and ETS transcription factor genes in prostate cancer. *Science* 2005;310:644–8.
- Tomlins SA, Mehra R, Rhodes DR, et al. *TMPRSS2:ETV4* gene fusions define a third molecular subtype of prostate cancer. *Cancer Res* 2006;66:3396–400.
- Ilijin K, Wolf M, Edgren H, et al. *TMPRSS2* fusions with oncogenic ETS factors in prostate cancer involve unbalanced genomic rearrangements and are associated with HDAC1 and epigenetic reprogramming. *Cancer Res* 2006;66:10242–6.
- Tomlins SA, Laxman B, Dhanasekaran SM, et al. Distinct classes of chromosomal rearrangements create oncogenic ETS gene fusions in prostate cancer. *Nature* 2007;448:595–9.
- Hermans KG, van Marion R, van Dekken H, Jenster G, van Weerden WM, Trapman J. *TMPRSS2:ERG* fusion by translocation or interstitial deletion is highly relevant in androgen-dependent prostate cancer, but is bypassed in late-stage androgen receptor-negative prostate cancer. *Cancer Res* 2006;66:10658–63.
- Lapointe J, Kim YH, Miller MA, et al. A variant *TMPRSS2* isoform and *ERG* fusion product in prostate cancer with implications for molecular diagnosis. *Mod Pathol* 2007;20:467–73.
- Mehra R, Tomlins SA, Shen R, et al. Comprehensive assessment of *TMPRSS2* and ETS family gene aberrations in clinically localized prostate cancer. *Mod Pathol* 2007;20:538–44.
- Rubin MA, Putzi M, Mucci N, et al. Rapid (“warm”)

- autopsy study for procurement of metastatic prostate cancer. *Clin Cancer Res* 2000;6:1038-45.
9. Glinsky GV, Glinskii AB, Stephenson AJ, Hoffman RM, Gerald WL. Gene expression profiling predicts clinical outcome of prostate cancer. *J Clin Invest* 2004; 113:913-23.
10. Lapointe J, Li C, Higgins JP, et al. Gene expression profiling identifies clinically relevant subtypes of prostate cancer. *Proc Natl Acad Sci U S A* 2004;101:811-6.
11. Vanaja DK, Chevillat JC, Iturria SJ, Young CY. Transcriptional silencing of zinc finger protein 185 identified by expression profiling is associated with prostate cancer progression. *Cancer Res* 2003;63: 3877-82.
12. Rhodes DR, Yu J, Shanker K, et al. ONCOMINE: a cancer microarray database and integrated data-mining platform. *Neoplasia* 2004;6:1-6.
13. Tomlins SA, Mehra R, Rhodes DR, et al. Integrative molecular concept modeling of prostate cancer progression. *Nat Genet* 2007;39:41-51.
14. Rhodes DR, Kalyana-Sundaram S, Tomlins SA, et al. Molecular concepts analysis links tumors, pathways, mechanisms, and drugs. *Neoplasia* 2007;9:443-54.
15. Demichelis F, Fall K, Perner S, et al. TMPRSS2:ERG gene fusion associated with lethal prostate cancer in a watchful waiting cohort. *Oncogene* 2007;26:4596-9.
16. Cai C, Hsieh CL, Omwancha J, et al. ETV1 is a novel androgen receptor-regulated gene that mediates prostate cancer cell invasion. *Mol Endocrinol* 2007;21: 1835-46.
17. Dechow TN, Pedranzini L, Leitch A, et al. Requirement of matrix metalloproteinase-9 for the transformation of human mammary epithelial cells by Stat3-C. *Proc Natl Acad Sci U S A* 2004;101:10602-7.
18. de Launoit Y, Chotteau-Lelievre A, Beaudoin C, et al. The PEA3 group of ETS-related transcription factors. Role in breast cancer metastasis. *Adv Exp Med Biol* 2000;480:107-16.
19. Soller MJ, Isaksson M, Elfving P, Soller W, Lundgren R, Panagopoulos I. Confirmation of the high frequency of the TMPRSS2/ERG fusion gene in prostate cancer. *Genes Chromosomes Cancer* 2006;45:717-9.
20. Wang J, Cai Y, Ren C, Ittmann M. Expression of variant TMPRSS2/ERG fusion messenger RNAs is associated with aggressive prostate cancer. *Cancer Res* 2006;66:8347-51.
21. Yoshimoto M, Joshua AM, Chilton-Macneill S, et al. Three-color FISH analysis of TMPRSS2/ERG fusions in prostate cancer indicates that genomic microdeletion of chromosome 21 is associated with rearrangement. *Neoplasia* 2006;8:465-9.
22. Clark J, Merson S, Jhavar S, et al. Diversity of TMPRSS2-ERG fusion transcripts in the human prostate. *Oncogene* 2007;26:2667-73.